Crystal Structure of Liganded and Unliganded Forms of Bovine Plasma Retinol-binding Protein*

Giuseppe Zanotti‡

*From the Department of Organic Chemistry, University of Padova and Biopolymer Research Center,
Consiglio Nazionale delle Ricerche, 35131 Padova, Italy*

Rodolfo Berni

From the Institute of Biochemical Sciences, University of Parma, 43100 Parma, Italy

Hugo L. Monaco

*From the Department of Genetics and Microbiology and Centro Interuniversitario per lo Studio delle Macromolecole
Informazionali, University of Pavia, 27100 Pavia, Italy*

The three-dimensional structures of bovine plasma retinol-binding protein (bRBP) complexed with retinol (space group P2₁2₁2₁, a = 46.08, b = 49.13, c = 78.10 Å) and of the unliganded protein prepared *in vitro* by extracting retinol with ethyl ether (space group P2₁2₁2₁, a = 46.55, b = 48.97, c = 78.67 Å) have been solved at 1.9 and 1.7 Å resolution, respectively. The final crystallographic R factors are 0.190 for holobRBP and 0.196 for the unliganded bRBP.

The model for the bovine holoprotein is quite similar to that of the human protein, with which it exhibits 92% sequence similarity. The root mean square deviation between the α-carbons in the two proteins is 0.31 Å. The retinol binding site is almost completely preserved. The loops that surround the opening of the β-barrel are also particularly conserved, in contrast with the presence of several substitutions in parts of the RBP molecule opposite the opening of the calyx that binds retinol.

Despite the fact that unliganded bovine RBP was prepared and crystallized using procedures completely different from those used to obtain the unliganded human RBP, the conformational differences between unliganded and liganded forms of bRBP are almost identical to those found previously between the same forms of human RBP. They mainly involve a few residues in the region extending from amino acid residues 32 to 37. Therefore, similar differences are very likely to exist between holoRBP and the physiologically occurring apoprotein. A not yet identified electron density, different in shape and orientation from retinol, also occupies the central cavity of the β-barrel in the unliganded bRBP, as found for unliganded human RBP. The functional consequences of the conformational change induced by the removal of retinol on the

interaction between RBP and transthyretin, coupled with the conservation of the entrance loops of the β-barrel in mammalian RBPs, are consistent with their participation in molecular interactions.

Retinol-binding protein (RBP),[1] the specific carrier of retinol in plasma, has been isolated from several vertebrates: mammals (Kanai et al., 1968, Muto and Goodman, 1972; Rask, 1974; Heller, 1975), chicken (Mokady and Tal, 1974), and fish (Shidoji and Muto, 1977, Berni et al., 1992). In every case, plasma RBP has been found to be a single polypeptide chain containing one single binding site for retinol. Its function is to transport the vitamin from the liver to specific cell surface receptors (Båvik et al., 1991), and it circulates in mammalian plasma bound to another protein, transthyretin, formerly called prealbumin, as a 1:1 molar complex (Goodman, 1984). Human plasma RBP is the variant that has been best characterized so far: its amino acid sequence is known (Rask et al., 1979), different crystal forms of the holoprotein and crystals of the apoprotein have been obtained (Ottonello et al., 1983; Newcomer et al., 1984; Monaco et al., 1984), and its three-dimensional structure has been solved by x-ray diffraction techniques (Cowan et al., 1990; Zanotti et al., 1993).

The bovine retinol-RBP complex (holobRBP) has molecular mass (21 kDa), amino acid composition, absorption and fluorescence spectra, and binding affinity to transthyretin very similar to those of the human complex (Heller, 1975; Berni et al., 1990). However, the bRBP-transthyretin complex has the peculiar property of being significantly dissociated when plasma proteins are run through an ion exchange DEAE-Sephadex column during the classical procedure used for the purification of RBP from most species (Berni and Lamberti, 1989). The amino acid sequence of bRBP has been found to be 92% identical to that of the human counterpart (Berni et al., 1990).

Following the crystallization of both liganded (Berni et al., 1990) and unliganded forms of bRBP in a crystal form very closely related to that of the human holoRBP that was used for a three-dimensional structure determination at 2.0 Å resolution (Cowan et al., 1990), we have extended the structural study to the bovine variant, with the aim of relating its

functional and structural properties. To this end, we describe here the structures of the unliganded, obtained by retinol extraction with organic solvent as opposed to the chromatographic procedure that led to unliganded human RBP (Zanotti et al., 1993), and liganded forms of bovine RBP. The structures of the two forms of bRBP have been refined to a nominal resolutions of 1.7 and 1.9 Å, respectively.

EXPERIMENTAL PROCEDURES

Purification and Crystallization of Liganded and Unliganded Forms of Bovine RBP

holobRBP was purified from bovine plasma as described (Berni and Lamberti, 1989). As the last step of this purification, a chromatography on a human transthyretin-Sepharose 4B affinity column (see below) was also used. The unliganded hRBP was prepared by extracting retinol from the holoprotein with ethyl ether, using the following procedure. The solution of holoRBP (10 ml in 20 mM Tris-HCl, pH 7.2) was thoroughly mixed with 2 volumes of the organic solvent at 2 °C for 20 min and the ethyl ether phase separated. This step was repeated twice. Finally, the ethyl ether remaining in the aqueous solution was evaporated under vacuum. After this treatment the protein was completely devoid of retinol, on the basis of the lack of the absorbance peak centered at 330 nm, which is characteristic of retinol bound to RBP. Both liganded and unliganded forms of bRBP at concentrations of 6–10 mg/ml were crystallized by microdialysis against 0.1 M sodium chloride, 0.01–1 mM cadmium acetate, 0.1 M sodium acetate buffer, pH 5.0–5.3. A summary of the crystal data is given in Table I.

Affinity Chromatography of Liganded and Unliganded bRBP

Approximately 10 nmol of bRBP samples were applied to a human transthyretin-Sepharose 4B affinity column (1 × 5 cm, prepared as described (Berni et al., 1992) and equilibrated with 0.15 M sodium chloride, 0.005 M sodium phosphate, pH 7.0). Elution was performed at a 0.2-ml/min flow rate with a linear gradient from this buffer to 0.001 M sodium phosphate, pH 7.4, at room temperature.

X-ray Diffraction Data Collection and Processing

The conditions selected to prepare the derivatives used in the calculation of the multiple isomorphous replacement electron density maps are reported in Table II. The x-ray source for data collection was an Elliot GX20 rotating anode generator operated at 1.6 kilowatts (40 kV, 40 mA) with an apparent focus size of 0.2 × 0.2 mm. Rotation photographs were taken on a Arndt-Wonacott Nonius FR553 camera using nickel-filtered copper radiation and a 0.5-mm collimator. Crystals were rotated 90° around the c axis, except for one native crystal, mounted with the b crystallographic direction parallel to the camera spindle. Four crystals were used for the native data set, with a crystal to film distance of 55 mm and a rotation range of 2°/picture. The derivative data were collected using one single crystal in each case, with a crystal to film distance of 75 mm.

The diffraction photographs were scanned on a rotating drum Optronics P1000 densitometer, operated by a PDP 11/34 computer.

Intensities were evaluated using the program SCAN12 (Crawford, 1977), and data were then scaled and merged using the program ROCKS (Reeke, 1984). Partially recorded reflections and those having intensities less than 1σ(I) were discarded.

To improve the resolution of the holoprotein, a native data set was collected using synchrotron radiation at the EMBL outstation Hamburg. The conditions used were: wavelength 1.400 Å, crystal to film distance 58.5 mm, average exposure time per photograph 900 s, 2° oscillation pictures were taken from a crystal mounted with the c axis along the spindle, and 1° pictures from another mounted with the b axis on the spindle, for a total of 24 and 42 exposures, respectively. Intensities were evaluated with the program MOSFLM (Nyborg and Wonacott, 1977) and data merged with the program AGROVATA contained in the CCP4 package. The two native data sets of the holoprotein, the one collected with the rotating anode and the other with synchrotron radiation, were not merged, and only the second was used in the last stages of the refinement.

Data for the unliganded protein were collected on a Siemens multiwire proportional counter area detector and processing was done using the XENGEN software package (Howard et al., 1985). 0.25° frames were collected on a three-axis goniometer. The x-ray source was a Rigaku RU-200 rotating anode generator run at 40 kV and 120 mA, with an apparent focusing size of 0.3 × 0.3 mm. Table III summarizes data collection and processing statistics and gives the percentage of reflections measured as a function of resolution for the native data sets.

Multiple Isomorphous Replacement

Three-dimensional difference-Patterson maps were calculated at 3.0 Å resolution. The KAu(CN)₂ derivative could be interpreted in terms of one major site, and cross-difference Fourier maps yielded the positions of the heavy atom sites of the other derivatives.

The positions of the heavy atom sites were refined using the standard phase refinement procedure (Blow and Crick, 1959). A summary of the heavy atom parameters and the phasing statistics is given in Tables IV and V, respectively. The overall figure of merit was $\langle m \rangle = 0.57$ for reflections at 3.0 Å resolution.

Model Building and Refinement

holobRBP—A Fourier map of the crystals of holobRBP at a nominal resolution of 3 Å was calculated with a grid sampling of approximately 1 Å, using set 1 of native data (see Table III) and the isomorphous phases weighted by the figure of merit (Blow and Crick, 1959). The Rice University version of the FRODO model building program (Jones, 1978; Pflugrath et al., 1984), running on an Evans and Sutherland PS300 interactive graphic system connected to a microVAX 3100 computer, was used for the display of the maps. A preliminary interpretation of the electron density was possible by using the chain trace of the model built for human RBP in the trigonal crystal form. Crystallographic refinement was performed alternating cycles of reciprocal space restrained refinement and manual rebuilding of the model. The restrained least squares procedure developed by Hendrickson and Konnert was adopted (Konnert, 1976; Hendrickson, 1985). In the first stages of the refinement, maps with coefficients $2F_{obs}-F_{calc}$ and combined multiple isomorphous replacement-calculated phases (Sim, 1959; Hendrickson and Lattman, 1970) were used. Subsequently, only calculated phases and the native data set collected using synchrotron radiation (denoted as set 2 in Table III) were used. At this stage the coordinates of human holoRBP, kindly provided by Dr. T. A. Jones, were used, after substitution of the amino acids that are different in the two sequences. The model was adjusted using the minimization program of the X-PLOR package (Brünger et al., 1987) and subsequently refined with the restrained least squares program TNT (Tronrud et al., 1987). With regard to the retinol molecule, restraints were applied only to bond distances and valence angles but not to torsion angles. In the final cycles of refinement, individual temperature factors were refined, without constraints. Solvent molecules were introduced in correspondence of peaks with high electron density and close to polar side chains or to other water molecules. The solvent structure was periodically revised, and all of the water molecules with high thermal parameter were excluded, and other added. The final crystallographic R factor for the holoRBP model is 0.190 for 12,126 observed reflections ($I > 1\sigma(I)$) between 9.0 and 1.9 Å.

Unliganded bRBP—The above model, from which the bound retinol was removed, was used as the starting point for the refinement of the unliganded form of bRBP. After some cycle of minimization,

TABLE I
Crystal data

Space group $P2_12_12_1$, $Z = 4$, $V_m = 2.03$ Å³/Da.

HolobRBP	a = 46.69	b = 49.12	c = 76.10
Unliganded bRBP	a = 46.55	b = 48.97	c = 75.87

TABLE II
Preparation of heavy atom derivatives

The soaking was done at room temperature. In all cases the solution contained 0.1 M NaCl and 0.001 M CdCl₂.

Derivative and concentration	Soaking time	Conditions
	h	
KAu(CN)₂ (0.005 M)	48	0.1 M acetate, pH 5.0
K₂HgI₄ (0.002 M)	20	0.1 M acetate, pH 5.0
K₃IrCl₆ (0.01 M)	48	0.03 M sodium cacodylate, pH 6.8

TABLE III

Data collection and processing

Percentage of reflections was measured for native holo- and unliganded bRBP.

Dataset	No. of crystals	No. of measurements	No. of unique reflections	R_{merge}[a]	R	Resolution range	Native[b] holobRBP	%	Native unliganded bRBP	%
HoloRBP (1)[c]	4	48,405	10,239	0.069		∞–4.2	1,190	83	1,413	98
HoloRBP (2)	2	44,450	12,224	0.101[d]		4.2–2.7	3,761	94	3,965	99
Unliganded bRBP	3	70,544	13,382	0.169		2.7–2.3	3,670	94	3,888	99
KAu(CN)₂	1	9,089	6,492	0.040	0.102	2.3–2.0	2,387	92	2,513	97
K₂HgI₄	1	13,540	6,593	0.071	0.226	2.0–1.9	1,216	47	2,476	96
K₂IrCl₆	1	10,106	5,600	0.040	0.075	1.9–1.7			4,061	80
						∞–maximum resolution	12,224	77	18,316	95

[a] $R_{merge} = \Sigma |I_i - I_j|/\Sigma I_{av}$ where i is the intensity observed in the ith source and j the intensity in the jth source. R is the mean fractional isomorphous difference, calculated with the same formula, except that now i and j refer to native and derivative, respectively.

[b] Statistics refer to set 2 of native data for the holo form, collected using synchrotron radiation. Reflections are considered observed if $I > 1\sigma(I)$.

[c] Native set 1 refers to rotating anode data and set 2 to data collected using synchrotron radiation (see "Experimental Procedures" for details).

[d] The R_{merge} for the two crystals separately is 0.064 and 0.106 for crystals 1 and 2, respectively. 10,844 partial reflections were included in native set 2.

TABLE IV

Heavy atom parameters

Z is the site occupancy in electrons, on an approximately absolute scale. B is the isotropic temperature factor measured in Å². x, y, and z are the fractional coordinates in the crystal system.

Derivative and site	Z	x	y	z	B
KAu(CN)₂					
1	31.6	0.082	0.286	0.615	30.0
2	2.5	0.607	0.217	0.818	25.9
3	1.7	0.263	0.732	0.906	15.7
K₂HgI₄					
1	50.6	0.048	0.288	0.636	33.7
2	27.5	0.913	0.768	0.889	36.7
3	19.0	0.974	0.455	0.973	24.2
4	22.8	0.903	0.838	0.850	14.7
5	5.6	0.439	0.200	0.885	6.4
6	5.5	0.162	0.799	0.889	32.9
K₂IrCl₆					
1	20.5	0.209	0.739	0.758	40.8
2	3.7	0.279	0.613	0.752	24.9

an electron density map calculated with coefficients $|2F_{obs}-F_{calc}|$ showed clearly the movement of some amino acid side chains and an electron density, different in shape and orientation from retinol, inside the barrel. This density, tentatively attributed to solvent, was left uninterpreted. Several cycles of refinement were performed, and the protein model and the solvent were periodically revised. The final value of the R factor is 0.196 for 18,110 observed reflections between 9.0 and 1.7 Å. A summary of the statistics of the final model is given in Table VI.

RESULTS AND DISCUSSION

Bovine holoRBP Compared with Human holoRBP—The molecular structure of human RBP has been described extensively (Cowan et al., 1990; Zanotti et al., 1993). The model of the bovine holoprotein (Fig. 1) includes 1,597 atoms (1,411 protein atoms, 165 solvent molecules, and retinol). The final R factor is 0.190 for 12,126 observed reflections between 9 and 1.9 Å, with a final root mean square deviation from the ideal of 0.010 Å for bond distances and 2.9° for valence angles. Fig. 2a is a plot of the thermal parameters of main chain and side chain atoms as a function of the residue number. The mean B value for the main chain and the side chain atoms is 10.7 and 19.6 Å², respectively. These values are significantly lower than those observed for the human protein in the trigonal crystal form, and this can be partially ascribed to the higher solvent content in the latter crystal. The other factors that may influence these figures are the different level of resolution of the two structures and the different methods used for data collection. Nevertheless, a comparison of Fig. 2a of this paper with Fig. 4a of the paper by Zanotti et al. (1993) shows a good agreement in the behavior of the temperature factors. disordered or not well ordered regions involve amino acid residues 1 and 2, from 64 to 67, and from 171 to 173. Since the same areas are also disordered in the crystals of human RBP, it is reasonable to conclude that these correspond to intrinsically disordered areas of the protein. It

TABLE V

Multiple isomorphous replacement statistics

Root mean square $F_j = |\Sigma_h f_{hj}^2/n|^{1/2}$, where f_{hj} is the heavy atom scattering amplitude for reflection h of derivative j and n is the no. of reflections. The unit is electrons. Root mean square $E = \Sigma_h |\epsilon_{hj}/n|^{1/2}$, in which ϵ_{hj} is the lack of closure for reflection h of derivative j and n is the no. of reflections. The figure of merit is the mean value of the cosine of the phase angle error.

Derivative	No. of sites	Root mean square	Resolution range							
			8.9	6.4	5.2	4.4	3.8	3.4	3.0	Total
						Å				
KAu(CN)₂	3	F_j	54	51	50	44	39	33	28	38
		E	26	30	30	29	23	21	17	21
K₂HgI₄	6	F_j	149	121	95	80	73	66	53	79
		E	97	74	61	66	63	57	45	58
K₂IrCl₆	2	F_j	33	40	31	27	22	19	16	23
		E	27	23	32	23	23	20	20	21
Mean native amplitude			222	231	245	291	291	262	217	258
No. of reflections			85	144	295	498	584	730	939	3197
Figure of merit			0.69	0.73	0.72	0.65	0.54	0.53	0.50	0.57

is also important to notice that amino acids from 175 to 182 are neither visible in the electron density map in this structure nor in the other two crystal forms of human RBP. A Ramachandran plot (Ramachandran et al., 1963) presented in Fig. 3 shows that only Tyr-111 lies in a forbidden region, as it was observed for the same residue of the human protein. Moreover, only 5 residues of holobRBP, as compared with the human holoprotein, exhibit the conformational torsion angles of the left-handed α-helix, whereas for the sixth, Asn-65, the angles are φ = −86° and ψ = 11°. It is worth recalling that the chain around residues 65–66 is quite mobile and the electron density in the map not well defined.

The root mean square deviation of the α-carbon atoms of holobRBP versus the corresponding atoms of human holoRBP is shown in Fig. 4a. The root mean square deviation calculated for the corresponding α-carbons in the two molecules is 0.37 and 0.53 Å for the orthorhombic and the trigonal crystal forms, respectively. As expected, holobRBP compares better with the human protein in the same space group than with that in the trigonal crystal form. Nevertheless, the three structures are very similar (Fig. 5). The main significant differences between equivalent α-carbons are observed in regions 1–3, 62–68, and 142–149. The amino-terminal region is disordered in every crystal form, and our model has been built tentatively since no electron density can be observed for the side chains of amino acids 1 and 2. Another region in which the electron density is very poorly defined is that limited by amino acids 67–68. In the region 142–145, the chain connecting strand H to the α-helix, the amino acid sequence is quite different in the two proteins: 3 residues out of 5 change in bovine RBP as compared with the human protein (position 142: Ser → Asn; 144: Phe → Leu; 145: Ser → Pro). Particularly relevant are the modifications at positions 144–

145, where a bulkier Phe residue substitutes a smaller Leu and a Ser substitutes a Pro: the sequence Pro-Pro, present in the human molecule, is conformationally more rigid than Ser-Pro. The chain movements in this area (α-carbons are displaced about 1 Å from the previous position) are transmitted to the first turn of the helix, from residue 146 to 149. Finally, the carboxyl-terminal coil presents a small difference starting at residue 169, where a Pro substitutes a Val, and the displacement is transmitted until residue 173. A comparison of the bovine model with the trigonal form of human RBP also shows some differences in the area comprising residues 92–98, one of the loops surrounding the opening of the cavity.

Side chain orientation and conformation in the human and bovine models are in general fairly well preserved, particularly for hydrophobic residues. Amino acid side chains found in a different orientation in the two species are listed in Table VII. Residues different in the two sequences (Fig. 6) are found in most cases in similar conformations. A special case is represented by residue 52, which is a Gln in human and a His in bovine RBP, but the electron density does not fully account for a His side chain.

Most of the amino acid substitutions for mammalian RBPs are found in parts of the RBP molecule opposite the opening of the β-barrel (Berni et al., 1990). This finding tends to exclude the participation of these regions in molecular interactions (e.g. with transthyretin and cell surface receptors), as regions involved in such interactions are expected to remain especially conserved in the course of evolution. In fact, rat, rabbit, and bovine RBPs have been found to interact with human transthyretin (Poole et al., 1975; Shidoji and Muto, 1977; Berni et al., 1990), in agreement with the conservation of the transthyretin binding site on the RBP molecule. The observation that bRBP interacts with human and bovine transthyretin with the same binding affinity represents, indeed, strong evidence for the conservation to a high degree of the site that binds transthyretin in mammalian RBPs (Berni et al., 1990). In contrast with the presence of several amino acid substitutions in certain parts of the protein surface, the loops on the side of the opening of the β-barrel are especially conserved in mammalian RBPs, and at least one of them appears to participate in the interaction with transthyretin (see below). If we compare mammalian RBPs of known primary structure (human, rat, rabbit, and bovine RBPs), no amino acid substitutions are found in the above area, with the exception of amino acid differences at positions 65 (Asn → Ser) and 68 (Asp → Glu) for rat and at position 99 (Lys →

TABLE VI
Structure of the refined models

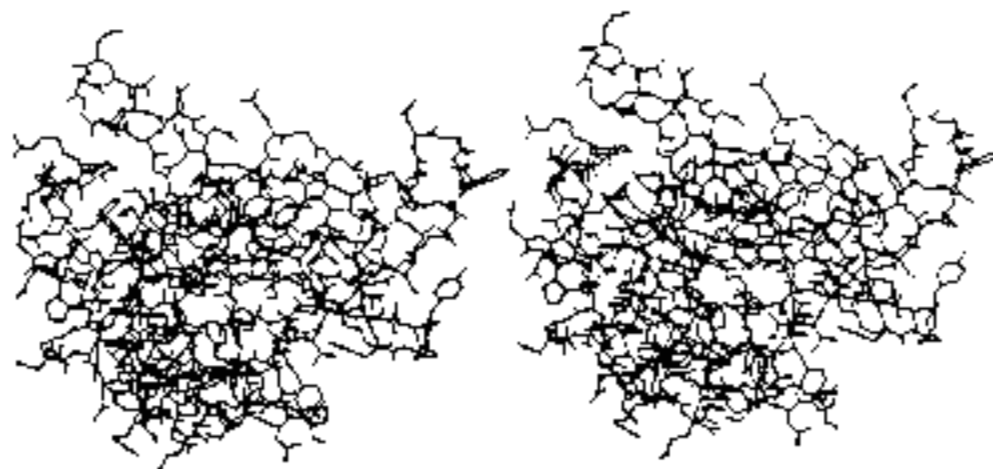|	HolobRBP	Unliganded bRBP
No. of reflections used	13,126	18,110
Resolution range	9–1.9	9–1.7
R factor	0.190	0.196
Root mean square deviations on		
Covalent bonds (Å)	0.010	0.011
Bond angles (°)	2.9	2.9
Planarity (Å)	0.008	0.008
Torsion angles (°)	26.2	26.3

FIG. 1. Stereo drawing of all of the atoms of holobRBP, from amino acid 1 to 174.
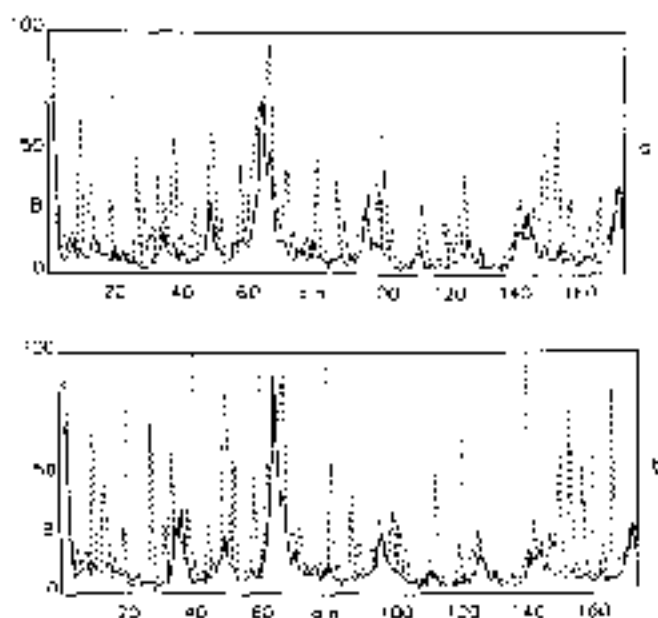
FIG. 2. **Mean thermal parameters (B, Å²) versus the amino acid number.** *Panel a*, holohRBP. Solid line, main chain atoms; dashed line, side chain atoms. *Panel b*, same as before, for unliganded bRBP.

FIG. 3. **Ramachandran plot of holo- (*panel a*) and unliganded bRBP (*panel b*).** *Squares* denote glycines; *crosses* indicate all of the others. The positions of the ϕ and ψ angles for amino acids 33–37, involved in the transition from the holo- to the unliganded form, are indicated.

Arg) for both rat and rabbit RBPs.

The retinol molecules in orthorhombic human RBP and bRBP are superimposed in Fig. 7 (the trigonal crystal form diffracts to lower resolution, and the model is not accurate enough for a detailed comparison of the vitamin position). Despite the fact that the two models superimpose quite well, differences are observed, particularly in the conformation of the cyclohexene ring. Whereas in human RBP (orthorhombic form) the torsion angle defined by the C5-C6 C7-C8 atoms, which is the angle defining the orientation of the tail with respect to the β-ionone ring, is 62°, in bRBP the value of the same angle is −165°. Both values have been reported in the literature for retinoids in the crystal state: a value of −166° is, for example, observed in the triclinic modification of retinoic acid (Stam, 1972). Moreover, the ring presents a slightly different conformation in the two molecules. Since the resolution of both structures is far from the atomic level, the small differences in the structure and orientation of the two vitamin molecules are perhaps attributable to the refinement procedure rather than to real differences in binding.

The interior of the protein is very well preserved in human and bovine RBPs. This high degree of conservation of the retinol binding site is also expected on the basis of the almost absolute conservation, among mammalian RBPs, of those amino acids that form the retinol binding site. If we compare human, rat, rabbit, and bovine RBP primary structures, no amino acid substitutions are found for the approximately 40 amino acid residues that take part in the formation of the retinol binding site, the only exception being the substitution at position 43 (Ala → Val) for rat RBP. It is interesting to note that in contrast with the above finding, several amino acid substitutions have been found for the same region in model structures of nonmammalian RBPs (Zapponi et al., 1992). However, the only allowed amino acid replacements for that region of nonmammalian as compared with mammalian RBPs are either conservative or more than 0.4 nm distant from retinol. Taken together, these findings indicate the existence of molecular constraints that are required to maintain structural features of the retinol binding site and to assure specificity and high affinity for the binding of retinol
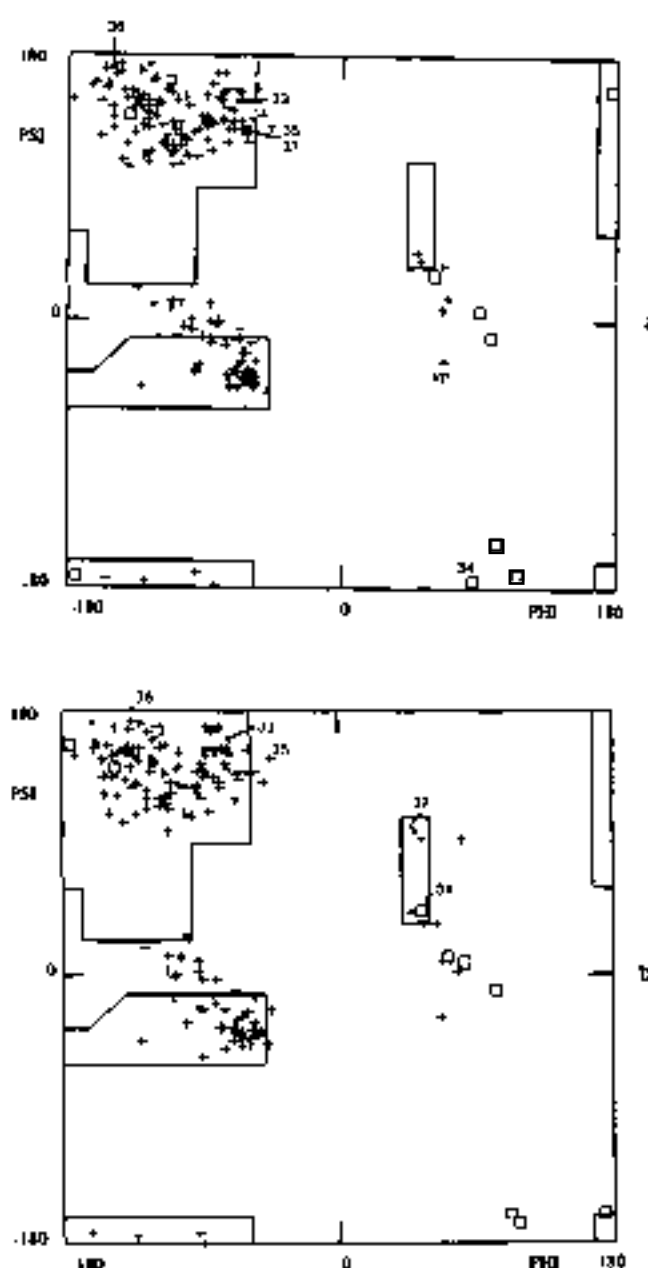
to its site in the RBP molecule.

Structure of the Unliganded Form of bRBP—The final model of unliganded bRBP has 1,589 atoms (1,422 protein atoms and 167 solvent molecules), with a root mean square deviation of 0.011 Å and 2.9° on bond lengths and valence angles, respectively. The mean temperature factors for the main chain and side chain atoms of the protein are 11.3 and 20.4 Å², respectively. Different from human RBP, mean temperature factors of the unliganded form are quite similar to those of the holo form, a fact that indicates that the absence of the specific ligand inside the β-barrel does not introduce disorder in the structure. Inspection of Fig. 2b, in which thermal parameters for the main chain and the amino acid side chain atoms are reported versus the residue number, indicates that regions that are relatively mobile in holobRBP

remain so in the unliganded form. The only exception is represented by the region comprising amino acids from 32 to 38, which in the holoprotein are quite fixed and in the unliganded protein present relatively high thermal parameters.

The model of unliganded bRBP is shown in Fig. 8, superimposed on that of holobRBP. The root mean square deviation is 0.71 Å between α-carbons of bRBP and 0.56 Å between the two unliganded proteins (Fig. 4b). It is evident from the figure that, excluding some small differences in the region from amino acid 61 to 68, which is a highly mobile area and not well defined in both proteins, the only real difference between the holoprotein and the unliganded model involves amino acids from 34 to 37. In particular, the amino acids that undergo a substantial conformational change are Leu-35 and Phe-36. This situation is very similar to that described for the liganded and unliganded forms of human RBP in the trigonal crystal form (Zanotti *et al.*, 1993). Fig. 9 illustrates

the movements of the two amino acids side chains: Phe-36, which in the holoprotein points toward the interior of the cavity, is positioned in the unliganded protein in the place previously occupied by the hydroxyl group of retinol; and Leu-35, because of a rotation of the main chain, points now clearly toward the exterior of the protein. This last movement is made possible by the absence of retinol in its binding site. The main chain torsion angles in this area for the human and bovine protein before and after the retinol release are summarized in Table VIII. It is interesting to notice that amino acids 35 and 36, the 2 residues significantly displaced from their previous positions, keep their original conformation, that is φ and ψ angles typical of the antiparallel β-strand. On the contrary, Leu-37 and Gly-34, which in the holoprotein are in a semiextended conformation, in the unliganded proteins assume the φ and ψ angles characteristic of the left-handed α-helix (see also Fig. 9, *a* and *b*). Moreover, from Table VIII it is evident that, neglecting small differences caused by the refinement procedure and by the different resolution, the conformational change from the holo to the unliganded RBP in the two crystal forms and in the two mammalian species is practically identical. Cowan *et al.* (1990) suggested that Leu-35 and Gln-98 might control the entrance and exit of retinol through the opening of the β-barrel and that a change in their side chain conformations should open up the binding site. Although on the basis of the two extreme models for the liganded and unliganded forms of RBP which we present we cannot exclude the occurrence of movements of Gln-98 side chain in the intermediate states that are associated with the transition from the holo to the apoprotein, our study indicates that the release of retinol involves the movement of the Leu-35 side chain and that the rotation of the main chain brings as a consequence a displacement of Phe-36 side chain. The former seems to be a movement necessary for the release of the vitamin, and the second, a consequence of that release. It is worth noticing that the only other relevant movement of side chains in the unliganded protein as compared with the holoprotein concerns Lys-29, whose side chain rotates around the Cβ-Cγ bond: the Nζ 29, which was previously forming a hydrogen bond with the carbonyl oxygen 37, now points in between oxygen 36 and 37.

The internal cavity of the β-barrel is not empty in the unliganded bRBP: significant maxima can be observed in the $|2F_{obs}-F_{calc}|$ and $|F_{obs}-F_{calc}|$ electron density maps (Fig. 10). It is difficult to explain this density in chemical terms, since the

FIG. 4. **Root mean square deviation (Å) of the equivalent α-carbons as a function of the residue number** for the models that are compared. *Panel a, solid line,* bovine holo- versus human holoRBP, orthorhombic crystal form; *dashed line,* bovine holo- versus human holo, rhombohedral crystal form. *Panel b, solid line,* bovine holo- versus bovine unliganded RBP; *dashed line,* bovine unliganded versus human unliganded RBP.
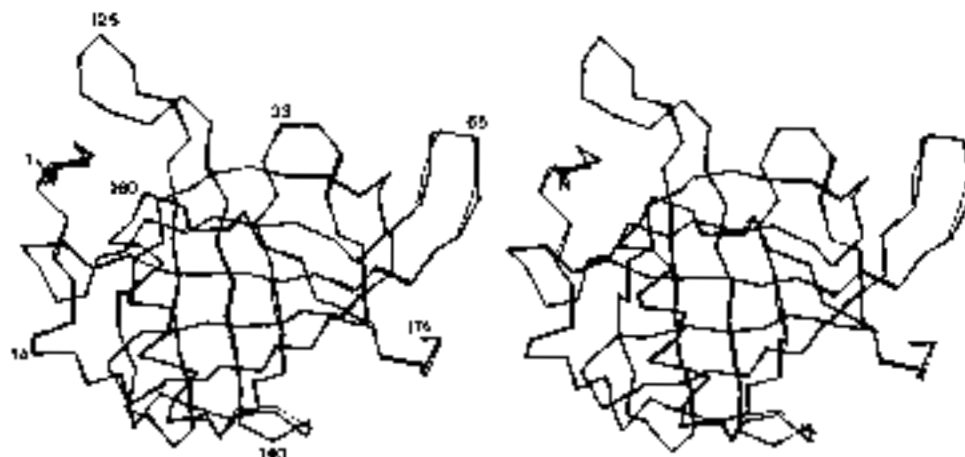

FIG. 5. **α-Carbon chain trace of the bovine holoRBP (*thick line*) superimposed to that of human holoRBP (*thin line*)** (Cowan *et al.*, 1990).

unliganded protein was produced by extracting the vitamin from holoRBP with ethyl ether, and the latter does not fully account, in shape and size, for the density we observe. It is important to notice that the electron density in the cavity is in contact, at one end, with Lys-29, suggesting the presence of at least a polar group in the molecules present in the retinol binding site. From the shape and the size of the density we cannot exclude the possibility that the cavity has been filled

by molecules other than ethyl ether, which were present in the solutions used for the extraction of retinol and the crystallization of unliganded RBP. The presence of a degradation product of the retinol molecule was excluded since the vitamin was quantitatively detected in the organic solvent after retinol extraction from holoRBP. The molecules that fill the cavity of the β-barrel are readily displaced by retinol, as a reconstituted holoRBP with the characteristics of the native holoprotein is obtained upon addition of retinol to the unliganded bRBP. In fact, the reconstituted retinol-RBP complex exhibits absorbance and fluorescence spectra (data not shown) and binding properties to transthyretin (Fig. 11) indistinguishable from those of the native holoprotein, thus indicating that the protein conformational changes that we have observed are completely reversible. Since we were not able to identify the molecules that replace the retinol in the β-barrel, we did not fit any molecular model to the density inside the cavity, although the addition of some ethyl ether molecules into it reduces the overall R factor from 0.196 to 0.192. It is also worth noticing that, according to the contour level selected in the electron density map, the shape and size of the density inside the cavity are quite similar to those found in unliganded human RBP (Zanotti et al., 1993). This finding, coupled to the fact that the two unliganded proteins were

TABLE VII

Amino acid side chains of bovine RBP which present a different orientation compared with equivalent chains of human RBP in orthorhombic crystal form

Amino acid side chain	Electron density	Interactions
Glu-33	Poor for Cβ and Cγ	
Glu-49	Very poor	Weak with water 578
Glu-81	Good	H-bond with water 272
Lys-87	Sufficient	Interactions with C = O 86 and OD2 103
Lys-89	Good	H-bond with water 312
Lys-99	Absent for Cγ and Nζ	
Lys-150	Good except for Cγ	
Arg-10	Good	H-bond with water 296
Arg-153	Poor from Cδ	
Arg-166	Poor for Cγ and Cδ	H bond with water 302 and 283

a

FIG. 6. *Panel a,* stereo view of the α carbons of holobRBP with superimposed the side chains of the amino acids that are different in the human protein. *Black circles denote* residues identical in human and bovine but different in rat or rabbit RBP. *Panel b,* amino acid sequence of bovine RBP (Berni *et al.,* 1990), with the residues that are different in human, rabbit and rat RBPs (Sundelin *et al.,* 1985). Features of secondary structure are indicated above the sequence of bovine RBP: a *continuous line* indicates a β-strand; *a dotted line* is the α-helix.

b

FIG. 7. **Vitamin binding site.** The retinol molecule in bovine RBP (*thick line*) is superimposed to the vitamin in the human protein (orthorhombic crystal form).
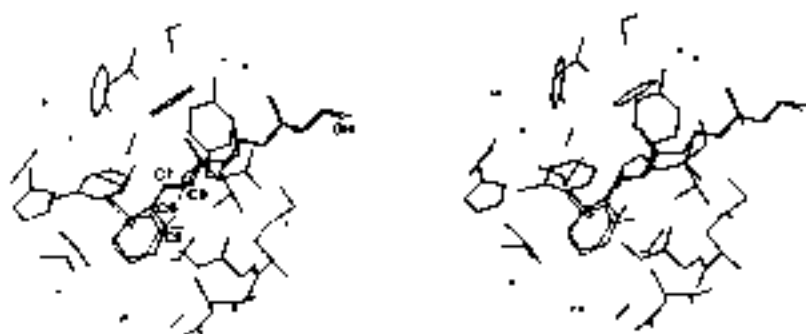
FIG. 8. **Stereo view of the α-carbon chain trace of the holo (*thick line*) and unliganded (*thin line*) proteins, superimposed.**
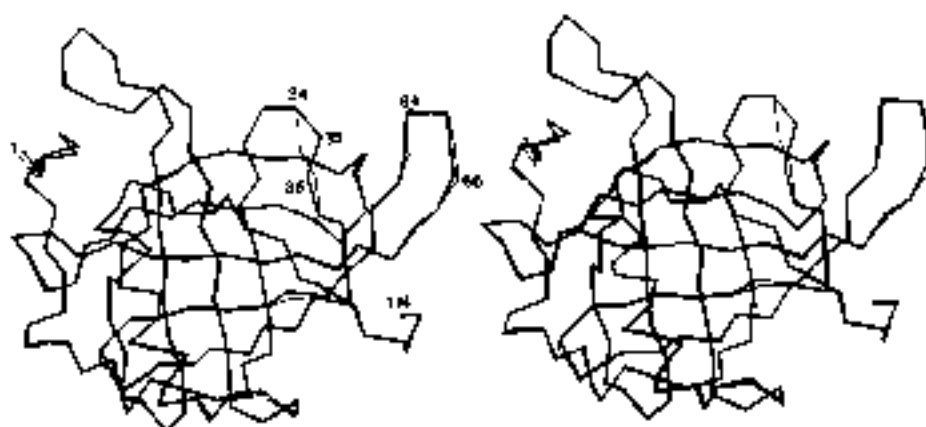
FIG. 9. *Panel a*, stereo view of the α-carbons of holo (*thick line*) and unliganded (*thin line*) bRBP, superimposed; all of the atoms of amino acid residues 35 and 36, which assume different positions in the two models, are shown. *Panel b*, model of unliganded bRBP, with the position of side chains of amino acids 35 and 36; the retinol molecule, drawn as it is present in the holoprotein, is in the position now occupied by the side chain of Phe-36.
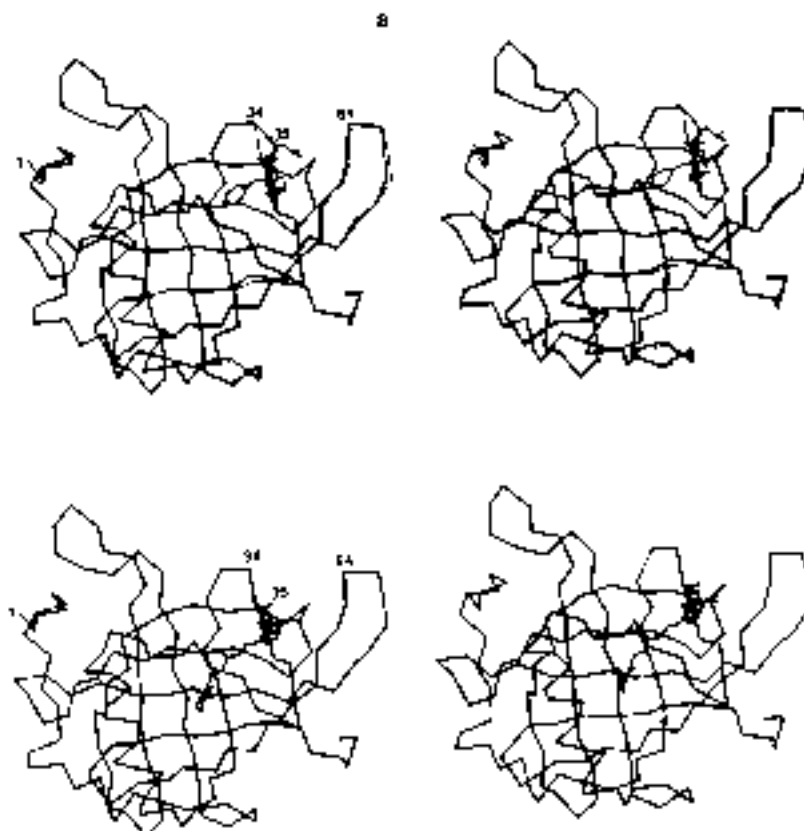
obtained and crystallized using completely different methods, tends to exclude that the density we observe represent contaminants of the solutions used for the removal of retinol from the holoproteins and for the crystallization of the unli-

TABLE VIII

Torsion angles of main chain atoms for the residues involved in the conformational transition from the holo to the unliganded form of RBP

Values for the human (hu)protein (Zanotti et al., 1993) are reported for comparison.

	HolohRBP		Unliganded bRHP		HolohRBP		Unliganded hRBP	
	φ	ψ	φ	ψ	φ	ψ	φ	ψ
Pro-32	−95	−108	−91	−170	−94	−170	−101	−177
Glu-33	−79	152	−75	155	−71	145	−65	151
Gly-34	87	−171	54	41	73	156	74	65
Leu-35	−68	130	−45	148	−54	132	−60	149
Phe-36	−145	169	−134	173	−164	161	−130	162
Leu-37	−63	131	54	93	−63	108	69	92
Gln-38	−91	−59	−89	−54	−76	−67	−81	−63

ganded proteins. One possible explanation of what we observe is that in both cases solvent molecules fill the cavity and, because of the lack of specific interactions, they are disordered and, therefore, of difficult identification. This conclusion is also supported by the relatively low level of the electron density we observe in the Fourier-difference map. Notably, the presence of water molecules in the β-barrel cavity has been established for apofatty acid-binding protein (Scapin et al., 1992). This finding further supports the possibility that solvent molecules also occupy the retinol binding site in the unliganded forms of human and bovine RBPs.

Interaction of the Unliganded bRBP with Transthyretin and the Transthyretin Binding Site in the RBP Molecule—The finding of similar conformational changes in both unliganded forms of human and bovine RBPs, obtained and crystallized using different procedures, with respect to holoRBP, suggests that similar conformational differences most probably exist between holoRBP and the physiologically occurring apoprotein. They are also presumably associated with the reported reduction in binding affinity to transthyretin of apoRBP as
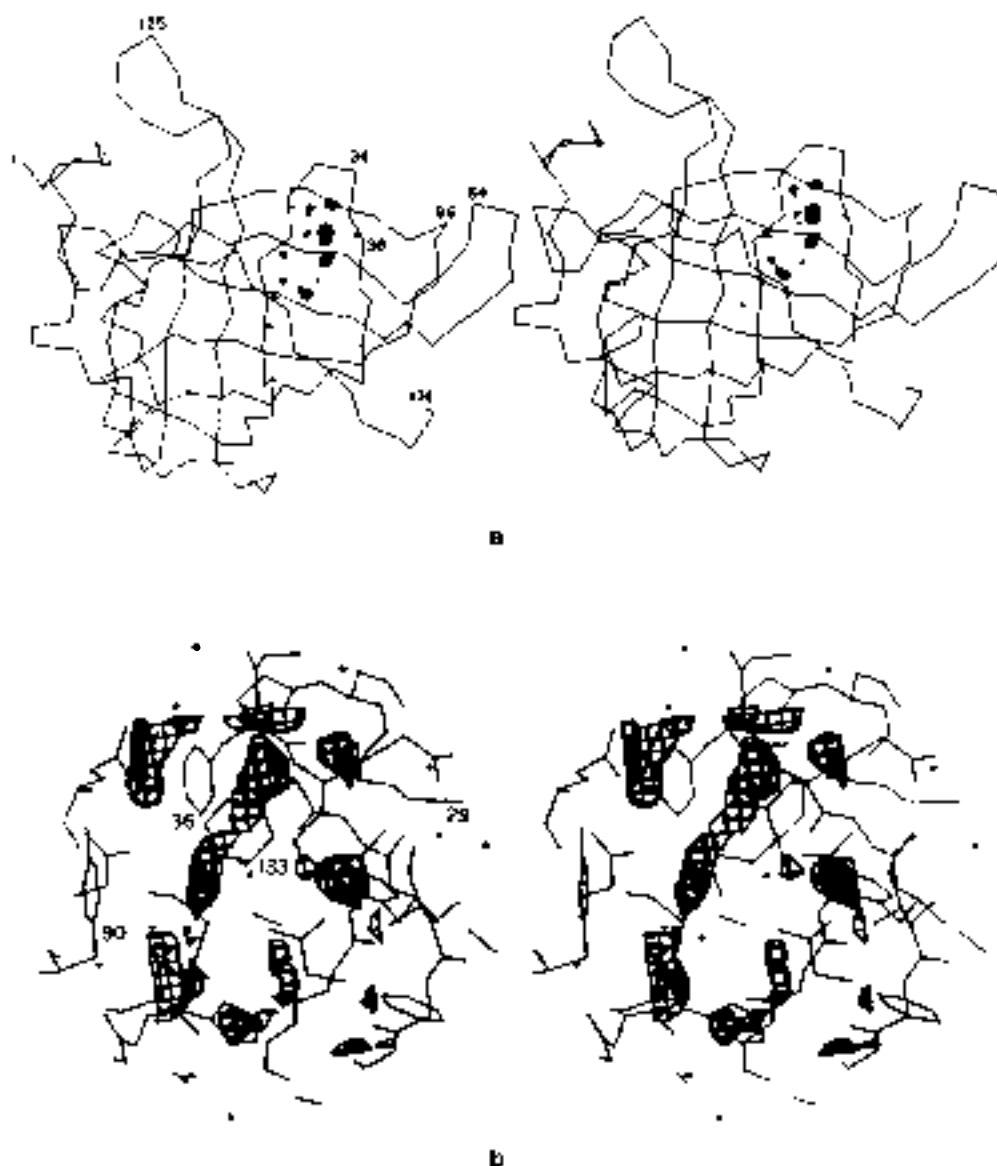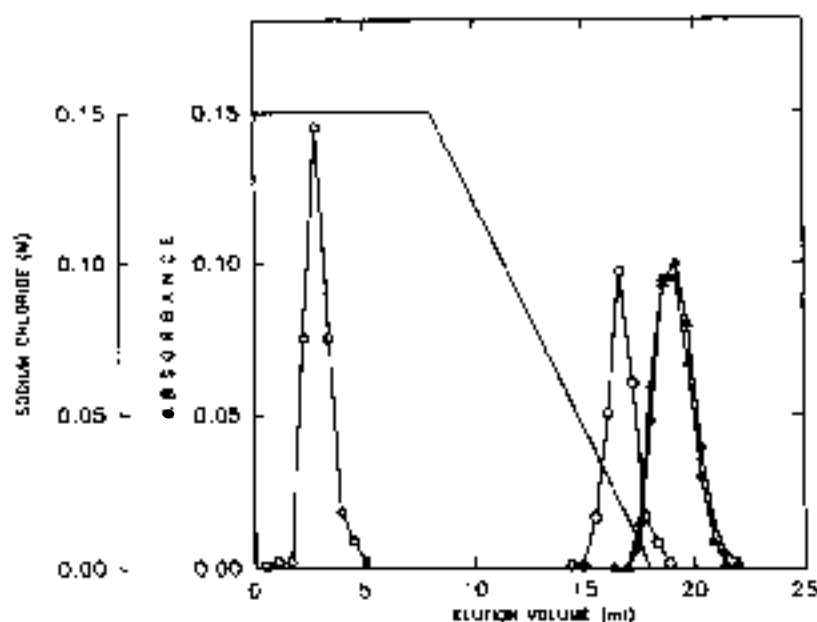

a

b

FIG. 10. *Panel a*, stereo drawing of the α-carbons of unliganded bRBP, with the electron density inside the cavity; electron density maps are calculated with coefficients |F_{obs}-F_{calc}|, contour levels at 2.5 σ. *Panel b*, a detail of the cavity, with the electron density calculated with coefficients |2F_{obs}-F_{calc}|, contour levels at 1.7 σ. Notice that Nζ of Lys-29 is close (2.6 Å) to one end of a maximum in the cavity.

compared with holoRBP (Raz *et al.*, 1970; Fex *et al.*, 1979). We have verified that the unliganded bRBP, obtained by retinol extraction with an organic solvent, exhibits distinct, although not remarkably different, elution profile as compared with liganded bRBP, when both forms are subjected to chromatography on a human transthyretin-Sepharose 4B affinity column (Fig. 11). Both forms are retained by the affinity matrix at high ionic strength (0.15 M NaCl). To obtain their desorption, the ionic strength must be reduced to very low values, as it was established for the human holoprotein (Vahlquist *et al.*, 1971). However, unliganded bRBP is eluted at approximately 20 mM NaCl, whereas the elution of the bovine holoprotein occurs at almost negligible ionic strength. As the chromatographic behavior is not remarkably different for both forms of RBP, their affinities for transthyretin may not be drastically different. Data reported in the literature estimated a dissociation constant for the human holoRBP-transthyretin complex not drastically lower than that of the human apoRBP (obtained from urine)-transthyretin complex (Fex and Hansson, 1979). Therefore, the quite limited conformational differences that we have found between liganded and unliganded bRBPs may be responsible for binding affinities to transthyretin not particularly different for the two RBP forms.

Finally, the finding that the conformational differences between the liganded and unliganded forms of bRBP are confined to a limited region of the RBP molecule, coupled to the observation that such changes affect the interaction with transthyretin, represents the strongest evidence obtained so far that the loop comprising residues from 32 to 37 is part of the site that binds transthyretin. Since this area is located at the entrance of the β-barrel, other loops of this zone might also interact with transthyretin. The hypothesis that these loops are involved in the interaction with transthyretin is also supported by other lines of evidence, namely their conservation in mammalian RBPs, molecular dynamics simulation for the transition from holo to apoRBP (Åqvist *et al.*, 1986), tryptophan labeling experiments (Horwitz and Heller, 1974; Cowan *et al.*, 1990), and the interference caused by the binding of retinoids to RBP on its affinity for transthyretin. With regard to the last point, RBP complexed with retinoids bearing bulky groups in place of the retinol hydroxyl group exhibits either reduced or no affinity for transthyretin (Berni *et al.*, 1993; Berni and Formelli, 1992), presumably as a result of structural changes induced by the retinoid binding to RBP which involve the entrance loops of the β-barrel. Åqvist and Tapia (1992) have recently proposed a possible molecular model for the RBP-transthyretin complex which is not incompatible with our structural data.

CONCLUSIONS

The crystal structures presented in this paper show that holobRBP, which is 82% homologous to the human protein, has a three-dimensional structure that is practically identical to that of the human holoprotein. Moreover, an unliganded bRBP, obtained *in vitro* by extracting retinol from the holoprotein with an organic solvent, exhibits the same, quite limited conformational change with respect to the holoprotein that was observed in an unliganded human RBP obtained in the course of protein purification (Zanotti *et al.*, 1993). The latter finding agrees with the observation that the unliganded human RBP (obtained by retinol extraction with ethyl ether) in solution at neutral pH is in a rigid state with properties similar to those of holoRBP (Bychkova *et al.*, 1992). Small molecules have been found to fill the interior of the β-barrel central cavity of both unliganded forms of human and bovine RBPs, obtained and crystallized using completely different methods. Despite the uncertain nature of the ligand that has substituted retinol in the two proteins, it is possible that they are different in the two cases, since the vitamin was extracted from the bovine protein with ethyl ether and from the human protein by exposure to hydrophobic matrixes. We cannot exclude that the limited movements and rearrangements of side chains we have observed depend on the nature of the molecules that substitute retinol and that apobRBP obtained using different procedures may display three-dimensional structures slightly different from those that we have determined. It is also debatable if the physiologically occurring apoprotein is similar or not to those obtained *in vitro*. In spite of these limitations, this structure, along with that of the unliganded form of human RBP, strongly supports the idea that the conformational change we observe is independent from the nature of the molecules that occupy the β-barrel cavity or of the method used for the extraction of the vitamin.

Moreover, the structures of the human and bovine unliganded proteins confirm that the β-barrel is very rigid and stable and that it can accommodate small molecules without gross alteration of its structure. At the same time, its rigidity prevents it from binding retinoids modified in the cyclohexene ring moiety (Berni *et al.*, 1990). On the contrary, the entrance of the β-barrel is a relatively flexible part of the protein, as demonstrated by the significant conformational change associated with the transition from the liganded to the unliganded form of RBP. This part of the molecule also appears to participate in the interaction with transthyretin. In conclusion, all of the evidence that we have presented suggests that the structure of the unliganded RBP we observe *in vitro* may be very similar to that of the RBP that has released retinol to cell surface receptors.

REFERENCES

Åqvist, J. and Tapia, O. (1992) *J. Mol. Graphics* **10**, 109–118
Åqvist, J., Sandblom, P., Jones, T. A., Newcomer, M. E., van Gunsteren, W. P., and Tapia, O. (1986) *J. Mol. Biol.* **192**, 593–604
Bávoil, C. O., Eriksson, U., Allen, R. A., and Peterson, P. A. (1990) *J. Biol. Chem.* **266**, 14985–14987
Berni, R., and Formelli, F. (1992) *FEBS Lett.* **308**, 43–45
Berni, R., and Lamberti, V. (1989) *Comp. Biochem. Physiol.* **94B**, 79–85
Berni, R., Stoppini, M., Zapponi, M. C., Meloni, M. L., Monaco, H. L., and Zanotti, G. (1990) *Eur. J. Biochem.* **192**, 507–513
Berni, R., Stoppini, M., and Zapponi, M. C. (1992) *Eur. J. Biochem.* **204**, 99–106
Berni, R., Zanotti, G., Sartori, G., and Monaco, H. L. (1983) in *Retinoids. Progress in Research and Clinical Applications* (Livrea, M. A., and Packer, L., eds.) pp. 91–100, Marcel Dekker, New York
Blow, D. M., and Crick, F. H. (1959) *Acta Crystallogr.* **12**, 794–802
Brunger, A. T., Kuriyan, J., and Karplus, M. (1987) *Science* **235**, 458–460
Bychkova, V. E., Berni, R., Rossi, G. L., Kurishenko, V. P., and Ptitsyn, O. B. (1992) *Biochemistry* **31**, 7566–7571
Cowan, S. W., Newcomer, M. E., and Jones, T. A. (1990) *Proteins Struct. Funct. Genet.* **8**, 44–61
Crawford, J. L. (1977) *High Resolution Structure of Aspartate Transcarbamylase*. Ph.D. thesis, Harvard University, Cambridge, MA
Fex, G., and Hansson, R. (1979) *Eur. J. Biochem.* **94**, 307–313
Goodman, D. S. (1984) in *The Retinoids* (Sporn, M. B., Roberts, A. B., and Goodman, D. S., eds.) vol. 2, pp. 41–88, Academic Press, New York
Heller, J. (1975) *J. Biol. Chem.* **250**, 6549–6554
Hendrickson, W. A. (1985) *Methods Enzymol.* **115B**, 252–270
Hendrickson, W. A., and Lattman, E. E. (1970) *Acta Crystallogr.* **B26**, 136–143
Horwitz, J., and Heller, J. (1974) *J. Biol. Chem.* **249**, 7181–7185
Howard, A. J., Nielsen, C., and Xuong, Ng. H. (1985) in *Methods Enzymol.* **114**, 452–472
Jones, T. A. (1978) *J. Appl. Crystallogr.* **11**, 268–272
Kanai, M., Raz, A., and Goodman, D. S. (1968) *J. Clin. Invest.* **47**, 2025–2044
Konnert, J. M. (1976) *Acta Crystallogr.* **A32**, 614–617
Muhady, S., and Tal, M. (1974) *Biochim. Biophys. Acta* **336**, 361–366
Monaco, H. L., Zanotti, G., Ottonello, S., and Berni, R. (1984) *J. Mol. Biol.* **178**, 477–479
Muto, Y., and Goodman, D. S. (1972) *J. Biol. Chem.* **247**, 2533–2541
Newcomer, M. E., Liljas, A., Sundelin, J., Rask, L., and Peterson, P. A. (1984b) *J. Biol. Chem.* **256**, 5925–5929
Nyburg, J., and Wonacott, A. J. (1977) in *The Rotation Method in Crystallography* (Arndt, U. W., and Wonacott, A. J., eds.) pp. 139–152, North Holland, Amsterdam
Ottonello, S., Maraini, G., Mammi, M., Monaco, H. L., Spadon, P., and Zanotti, G. (1983) *J. Mol. Biol.* **163**, 679–681
POatrash, J. W., Super, M. A., and Quiocho, F. A. (1984) in *Methods and Applications in Crystallographic Computing* (Hall, S., and Ashiaka, T., eds.) p. 407, Clarendon Press, Oxford
Poole, A. R., Dingle, J. T., Mallia, A. K., and Goodman, D. S. (1975) *J. Cell Sci.* **19**, 379–384
Ramachandran, G. N., Ramakrishnan, C., and Sasisekharan, V. (1963) *J. Mol. Biol.* **7**, 95–99
Rask, L. (1974) *Eur. J. Biochem.* **44**, 1–6
Rask, L., Anundi, H., and Peterson, P. A. (1979) *FEBS Lett.* **104**, 55–58
Raz, A., Shiratori, T., and Goodman, D. S. (1970) *J. Biol. Chem.* **245**, 1903–1912
Reeke, G. N. (1984) *J. Appl. Crystallogr.* **17**, 125–130
Scapin, G., Gordon, J. I., and Sacchettini, J. C. (1992) *J. Biol. Chem.* **267**, 4253–4269
Shidoji, Y., and Muto, Y. (1977) *J. Lipid Res.* **18**, 679–691
Sim, G. A. (1959) *Acta Crystallogr.* **12**, 813–815
Stern, C. H. (1972) *Acta Crystallogr.* **B28**, 2896–2945
Sundelin, J., Laurent, B. C., Anundi, H., Tragårdh, L., Lichamonius, D., Björk, I., Eriksson, U., Akergström, B., Jones, A., Newcomer, M., Peterson, P. A., and Rask, L. (1985) *J. Biol. Chem.* **260**, 6472–6480
Tronrud, D. E., Ten Eyck, L. F., and Matthews, B. W. (1987) *Acta Crystallogr.* **A43**, 489–501
Vahlquist, A., Nilsson, S. F., and Peterson, P. A. (1971) *Eur. J. Biochem.* **20**, 160–168
Zanotti, G., Ottonello, S., Berni, R., and Monaco, H. L. (1993) *J. Mol. Biol.*, in press
Zapponi, M. C., Zanotti, G., Stoppini, M., and Berni, R. (1992) *Eur. J. Biochem.* **210**, 937–943